ORIGINAL ARTICLE

Interactive 3D Hybrid PET/CT Imaging in the Identification of Myocardial Viability in Patients After Myocardial Infarction: Feasibility Study and Clinical Implications

*Yen-Wen Wu,[1,2] Wen-Jeng Lee,[3] Tzung-Dau Wang,[2] Wei-Te Lin,[4] Ruoh-Fang Yen,[2] I-Hui Wu,[5] Kai-Yuan Tzen,[2] Wen-Yih I. Tseng[3,6]**

Background/Purpose: Clinical decision-making in coronary artery disease requires integrated information on myocardial viability and coronary arteries, and cross-modality registration could facilitate this process. The recent emergence of hybrid positron emission tomography (PET)/computed tomography (CT) allows acquisition of this information in one study session; however, clinically useful software capable of presenting three-dimensional (3D) fused images to assess the relationship between myocardium and coronary arteries is limited.

Methods: Patients with prior myocardial infarction were examined using electrocardiographically gated 18F-fluorodeoxyglucose PET and 16-slice CT.

Results: There were seven patients; mean age was 59 ± 15 years and six were male. Using 3D reconstruction, coregistration and interactive display, the topographical relationship between myocardial viability and coronary arteries was clearly identified.

Conclusion: We present a protocol to acquire CT coronary angiography and PET data and to visualize 3D fused images with an interactive visualization interface. This image coregistration is potentially useful to facilitate the process of image interpretation and decision-making. [*J Formos Med Assoc* 2008;107(6): 470–477]

Key Words: computed tomography, coronary angiography, ^{18}FDG, ^{18}F-fluorodeoxyglucose, myocardial infarction, organ viability, positron emission tomography

Clinical decisions regarding diagnosis and treatment of coronary artery disease (CAD) require integrated information on coronary morphology and myocardial viability.[1] Current functional mapping of the myocardium often invokes a standard template of the coronary artery system to indicate the supplied myocardial segments of the left ventricle.[2] However, the standard template is only valid in 50–60% of patients,[3] thus mismatch between dysfunctional myocardium and significant coronary lesions is not uncommon.[4,5] Recent advances in multidetector spiral computed tomography (CT) provides a noninvasive means to assess coronary arteries with exquisite image quality.[6]

Departments of [1]Nuclear Medicine, [2]Internal Medicine, [3]Medical Imaging, [4]Medical Research, and [5]Surgery, National Taiwan University Hospital, and [6]Center for Optoelectronic Biomedicine, National Taiwan University College of Medicine, Taipei, Taiwan.

Received: February 26, 2007
Revised: April 10, 2007
Accepted: June 5, 2007

***Correspondence to:** Dr Wen-Yih I. Tseng, Department of Medical Imaging, National Taiwan University Hospital, and Center for Optoelectronic Biomedicine, National Taiwan University College of Medicine, 1 Jen-Ai Road, Section 1, Taipei 220, Taiwan.
E-mail: wytseng@ha.mc.ntu.edu.tw

Hybrid positron emission tomography (PET)/CT scanners make integrated mapping of the myocardium and coronary arteries feasible. Although cross-modality fusion has been reported,[7–10] challenges still remain in effective visualization to delineate relationships between the myocardium and coronary arteries.[11,12]

We present a PET/CT angiography acquisition protocol, image fusion and validation in seven patients with prior myocardial infarction (MI). The aims were to study the feasibility of integrated imaging of the coronary arteries and myocardial viability, and to determine its value in image interpretation and decision-making.

Patients and Methods

Patients

We consecutively studied seven MI patients who had nonreversible perfusion defects on dipyridamole-reinjection thallium-201 (^{201}Tl) single photon emission computed tomography (SPECT) within 1 month and were referred for ^{18}F-fluorodeoxyglucose (FDG)-PET. Patients with irregular heart rate, unstable condition, contraindications against iodinated contrast medium, or serum creatinine ≥ 1.5 mg/dL were excluded. The study was approved by the Research Ethics Committee of our hospital. Informed consent was given by patients before the study.

Dipyridamole ^{201}Tl-SPECT

Dipyridamole (0.56 mg/kg over 4 minutes) was intravenously infused. Three minutes later, 2–3 mCi ^{201}Tl was injected and SPECT was performed 5 minutes and 4 hours later. Subjects with nonreversible defects on the 4-hour images had 1 mCi ^{201}Tl injected and a set of SPECT was obtained 15 minutes later.[13] Images were interpreted using a 17-segmental model[2] and 0–4 scale (0 = normal to 4 = absent photon counts).[13,14] All subjects had ≥ 2 continuous segments of nonreversible perfusion defects of scale 3 or 4.

FDG-PET

FDG-PET and coronary CT angiography (CTA) were acquired using a hybrid PET/16-slice CT scanner (Discovery LS; GE) (Figure 1). After fasting for 4–6 hours, nondiabetic patients received 50 g of

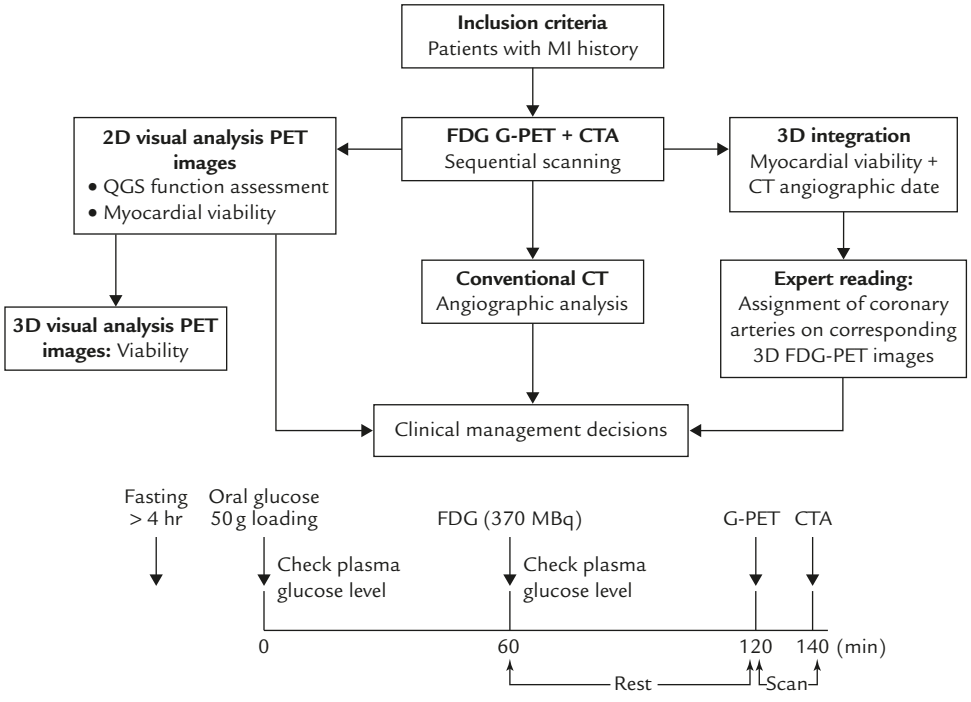

Figure 1. Protocol of the ^{18}F-fluorodeoxyglucose (FDG) positron emission tomography (PET) and coronary computed tomography angiography (CTA) study. G-PET = electrocardiographically-gated PET; 3D = three-dimensional; 2D = two-dimensional.

glucose orally while diabetic patients received soluble insulin intravenously according to blood glucose levels ≤ 115 mg/dL.[14] Sixty minutes later, 9–10 mCi FDG was administered. Patients received a scan 1 hour later. CT for transmission was performed (scan length, 15 cm; rotation time, 0.5 seconds; total acquisition time, 3.3 seconds; tube voltage, 120 kV at a current of 80 mA). PET was acquired in two-dimensional (2D) mode with ECG-gating (8 frames/R-R).

Coronary CTA

Coronary CTA was performed after PET without changing the patients' positions. Patients who had heart rate (HR) ≥ 65 bpm took oral beta-blockade (20–30 mg propranolol) 60 minutes earlier.[15,16] Nitroglycerin (0.8 mg) was administered sublingually if systolic blood pressure was ≥ 120 mmHg and HR ≤ 64 bpm. A bolus of 15–20 mL of contrast (Ultravist, 370 mg I/mL; Schering, Germany) was injected through the antecubital veins at a speed of 3–4 mL/s to determine transit time. Retrospective ECG-gated coronary CTA was performed (rotation time, 0.5 seconds; detector collimation, 16 × 0.625 mm; tube voltage, 120 kV at a current of 400 mA). A total of 65–80 mL of contrast was injected (adjusted by body weight) followed by 50 mL saline chaser.[15]

Three-dimensional (3D) PET/CT image reconstruction and processing

PET data were processed with a PC workstation (Xeleris, GE). Iterative reconstruction and CT-based attenuation correction were performed and reconstructed using an image matrix of 512 × 512, slice interval of 3.27 mm and thickness of 3.75 mm. CT data were processed with a conventional algorithm. If HR was ≤ 60 bpm, CTA was constructed at 75% of R-R by a single-sector segmented reconstruction algorithm. If HR was > 60 bpm, CTA was constructed at 45% and 75% of R-R using a two-sector segmented reconstruction algorithm (Advantage Windows 4.2; GE).[16] PET/CT registration was performed using graphics software (Amira v3.1; Mercury Computer Systems, MA, USA) by using CT images at 75% of R-R and PET at the sixth cardiac phase (62.5–75% of R-R). We used volume rendering of both images to identify the cardiac structures, and manually selected anatomical landmarks at the right ventricle insertion, papillary muscles in the mid-ventricular plane and apex as reference (Figure 2).

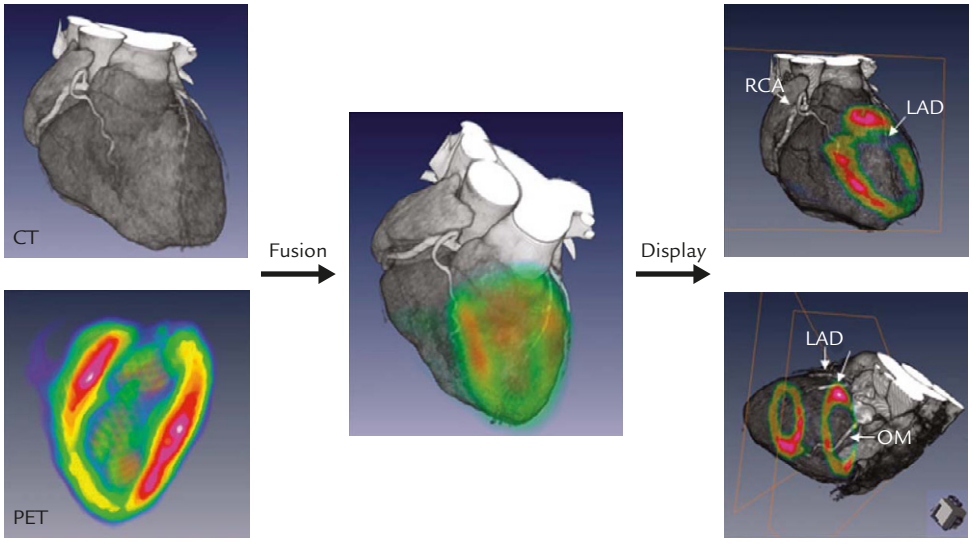

Figure 2. Positron emission tomography (PET)/computed tomography (CT) image fusion. CT images selected at 75% of the cardiac cycle and gated PET images of the sixth cardiac phase, equivalent to 62.5–75% R-R interval, were used for 3D reconstruction and registration with a 3D navigation scheme. CT coronary angiograms were rendered using 3D-texture volume rendering. Interactive visualization was achieved. RCA = right coronary artery; LAD = left anterior descending artery; OM = obtuse marginal artery.

Interactive visualization of fused PET/CT and interpretation and analyses

All images were reviewed by two independent readers, blind to patients' identities. PET was analyzed using a 17-segment model and 0–4 scale system, the same as SPECT. Segments with marked reduction or absence of FDG uptake (i.e. scales of 3–4) were classified as nonviable.[14] The method allowed viewing of cross-sectional PET images in any arbitrary orientation and position.

The image quality of CTA was assessed based on the presence of motion artifacts and vessel calcification, and graded as excellent (no motion artifacts), good (minor artifacts), moderate (substantial artifacts, but luminal assessment of significant stenosis still possible), heavily calcified (vessel lumen obscured by calcification), or blurred (only contrast visualization inside the vessel possible, no lumen assessment of significant stenosis possible). The presence of significant coronary (≥ 50%) or high grade lesions (≥ 90% stenosis) was evaluated visually with a 16-segment model.[17]

SPECT and PET were evaluated side-by-side in 2D and 3D display. Defects in the anterior and septal walls were allocated to the left anterior descending artery (LAD); defects in the lateral wall to the left circumflex artery (LCX); and inferior defects to the right coronary artery (RCA). The apex was considered to be LAD, unless defects extended to the lateral (LCX) or inferior walls (RCA).[3] Additional value of 3D fusion was defined if one of two investigators recorded it to be helpful.[5]

Results

The clinical characteristics and findings of SPECT, PET and CT are listed in the Table. Six patients had ST elevated MI (STEMI), and five received primary coronary intervention within 6 hours after chest pain. Three patients had one-vessel disease (VD), three patients had two-VD and one had three-VD. All examinations were complete without complications.

Image analyses

All had HR < 65 bpm and had moderate or better CTA image quality. Five patients had calcified plaques and three had stents. PET image quality was adequate for interpretation, including one with diabetes. There were four patients (Cases 2, 4, 6, 7) with a transmural scar on FDG-PET; three were allocated to LAD and one to LCX. The discrepant viability results using SPECT or PET were all confined to the inferior walls (Cases 1, 2, 3, 5), probably due to diaphragmatic attenuation.

3D fusion images and interactive visualization

All PET/CT images were successfully registered. Visual inspection by two observers indicated excellent matching on CT and PET in all cases. The infarct-related or significantly stenotic coronary lesions were clearly identified on coronary CTA in the four cases with scar. The assignment of the infarct-related arteries was consistent in the 2D and 3D displays. One reader found that in one out of seven patients (Case 2), 3D fusion images facilitated visual assignment. Two readers agreed that 3D provided a better estimation of infarct size, especially at the basal level.

Clinical management

All imaging findings were made available to the clinicians. Two patients underwent coronary angiography. In Case 3, significant in-stent restenosis in the RCA was disclosed and percutaneous transluminal balloon angioplasty was performed. In Case 5, stenting was performed at the LAD restenosis site.

Coronary angiography was not performed for nonsignificant coronary lesions (≤ 50%) on CTA (Cases 1, 2, 4, 6) and for a nearly transmural scar in infarct-related vascular territory (Cases 4, 6). In Case 7, CTA was consistent with the coronary angiogram of acute MI 2 years previously. Intervention was not performed because of essential thrombocytosis. The results of CTA and FDG-PET showed no recurrent coronary thrombosis or infarction since then (Figure 3).

Table. Demographic information and findings of single photon emission computed tomography (SPECT), coronary computed tomography angiography (CTA) and positron emission tomography (PET) for the seven patients

Case	Age (yr)	Sex	Prior MI	History of PCI	SPECT	Coronary CTA	PET	LVEF (%) by 2D-UCG
1	76	M	Anterior MI (NSTEMI no t-PA/primary PCI)	None	Fixed defect in inferior wall	Proximal LAD: calcified plaque, nonsignificant stenosis	Global viable	60
2	68	M	Lateral MI (STEMI s/p primary PCI)	LCX, RCA	Fixed defect in inferior & lateral walls	Distal LM-mid LAD: multiple calcified plaques, 50% stenosis	Decreased FDG uptake in mid to basal inferolateral wall	44
3	56	M	Inferior MI (STEMI s/p primary PCI)	RCA	Fixed defect in inferior wall	LAD-Dx bifurcation: plaque with non-stenotic lesion. Mid to distal RCA: decreased contrast enhancement below stent suggestive of significant in-stent stenosis	Global viable	50
4	54	M	Anterior MI (STEMI s/p primary PCI)	LAD	Fixed defect in apex, anterior wall & septum	No significant coronary stenosis; myocardial thinning with late enhancement in apex, anterior wall & septum	Nearly absent ^{18}FDG uptake in apex, anterior wall & septum	40
5	74	F	Inferior MI (STEMI s/p primary PCI)	LAD, RCA	Fixed defects in inferior wall	Mid LAD-proximal D2: mixed soft & calcified plaque with significant stenosis	Global viable	58
6	51	M	Anterior MI (STEMI s/p primary PCI)	LAD	Fixed defect in apex & anterior wall	Distal LCX, OM: 50% stenosis	Nearly absent ^{18}FDG uptake in apex & anterior wall	32
7	36	M	Anterior MI (STEMI no t-PA/primary PCI)	None	Fixed defect in apex, anterior & anteroseptal walls	Mid LAD: nearly total occlusion	Severe ^{18}FDG reduction in apex, mid anterior & anteroseptal walls	60

MI = myocardial infarction; PCI = percutaneous coronary intervention; LVEF = left ventricular ejection fraction; 2D-UCG = 2D-echocardiography (modified Simpson's method); NSTEMI = non ST-elevation MI; LAD = left coronary descending artery; STEMI = ST-elevation MI; LCX = left circumflex artery; RCA = right coronary artery; LM = left main; ^{18}FDG = ^{18}F-fluorodeoxyglucose; Dx = diagonal branch; OM = obtuse marginal branch.

Discussion

A hybrid PET-CT scanner can provide coronary and myocardial information simultaneously, and integration of PET/CT allows mapping of myocardial metabolism onto cardiac morphology. We show a new interactive visualization interface to view the registered PET/CT, which additionally offers clear topographical relationships, and is potentially useful in interpretation and decision-making.

Fusion images of coronary CTA with perfusion PET[7,8] or SPECT[9,10] have been previously described. Coronary CTA could reduce the misdiagnosis of scintigraphic studies in balanced ischemia and large fixed perfusion defects in patients with non-ischemic cardiomyopathy or soft tissue attenuation.[13,14] Data acquired in CTA can also be used to evaluate left ventricular function and regional wall motion, especially to assist in areas of decreased tracer activity. Scintigraphic data are helpful particularly in severe calcification, intermediate stenosis with functional relevance, stents or arrhythmia and motion artifacts during CTA.[7,18] We found that multivessel disease, coronary calcification and stents were common and scintigraphy could decrease diagnostic uncertainty. Our results also suggested that this approach might facilitate the diagnostic process, and better estimate the extent of the scar.

Recently, PET/CT and SPECT/CT systems have been shown to provide complementary information in one examination session.[8–10,18] Reliable post-processing procedures and image displays for clinical use become important in increasing the use of a multimodality approach. To minimize misregistration, we chose comparable cardiac phases and anatomical landmarks on PET/CT. As interactive identification of control points on two images is difficult and often a source of error,

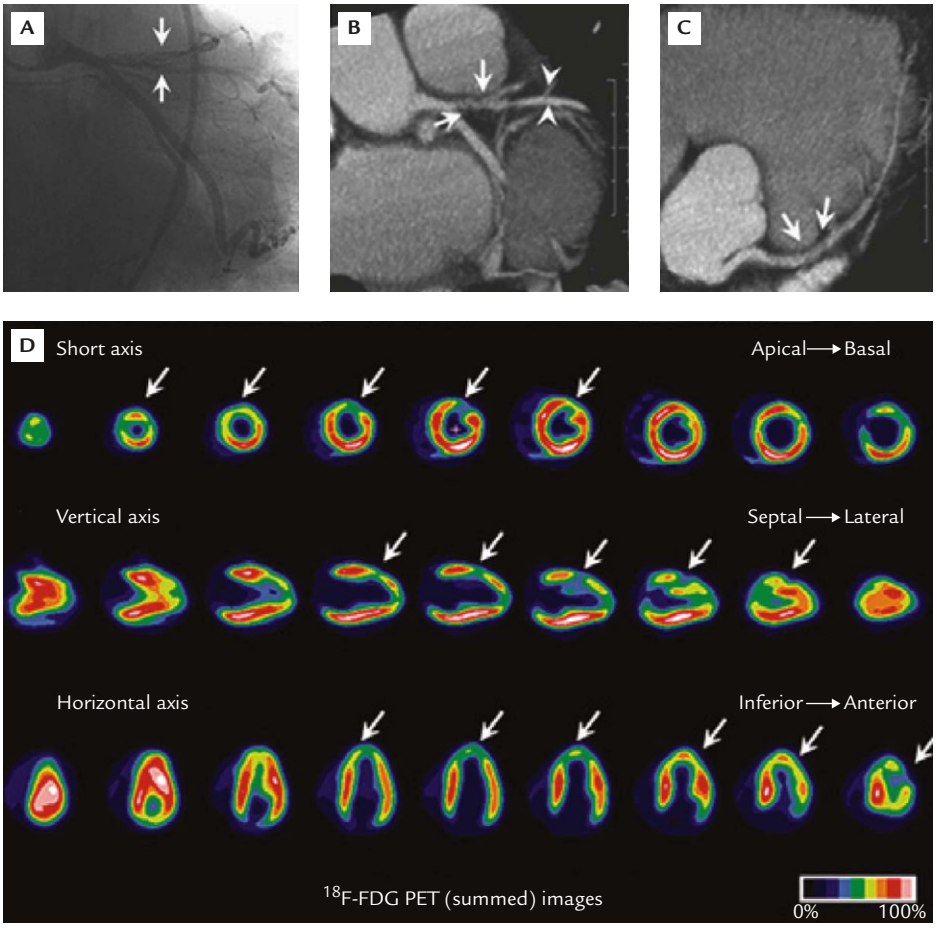

Figure 3. Continued

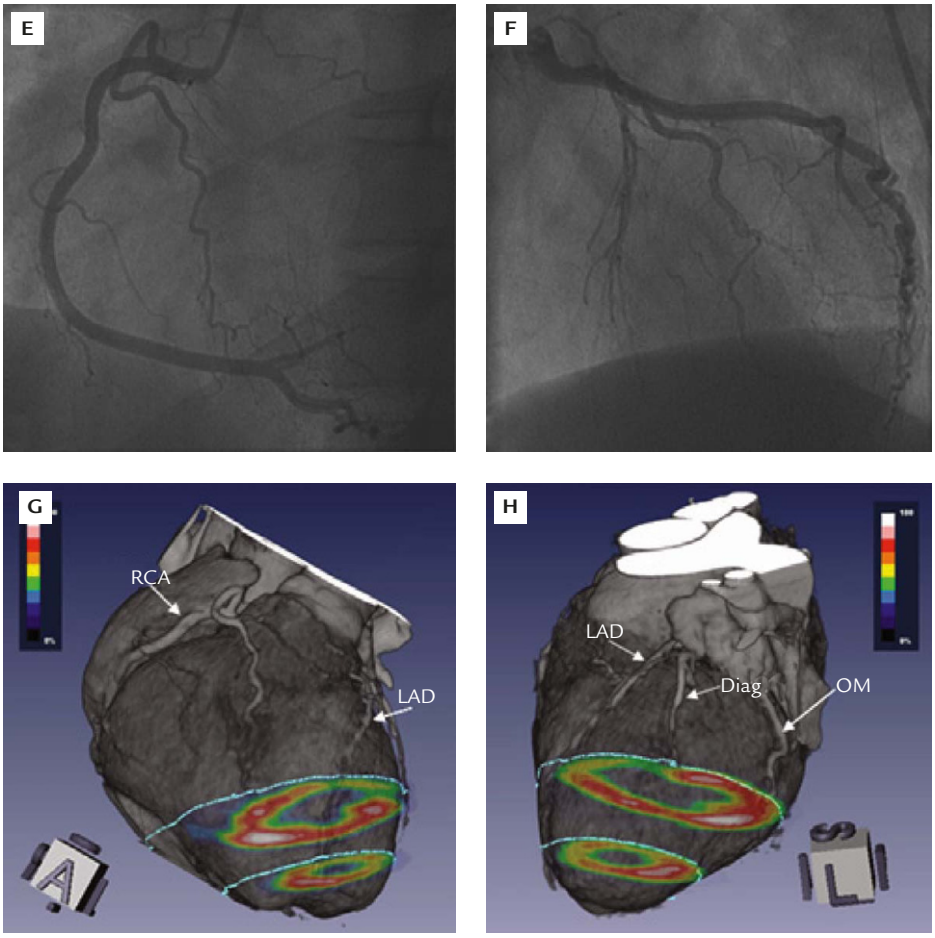

Figure 3. Example of a 35-year-old man with a history of anterior myocardial infarction 2 years previously. (A) Coronary angiogram in spider view discloses filling defects in the left anterior descending artery (LAD) and diagonal branch (arrows). (B, C) Coronary computed tomography angiography reveals significant stenosis with heterogeneous thrombi in the proximal to mid portion of the LAD (arrows) and diagonal branch (arrowheads). Faint and irregular contrast enhancement in the distal segment suggests spontaneous recanalization. Onsite ECG showed normal sinus rhythm with average heart beat of 56 bpm. Images were constructed at 75% of the R-R interval. (D) Positron emission tomography (PET) images in short, vertical and horizontal axes show severe reduction of ^{18}F-fluorodeoxyglucose (^{18}FDG) uptake in the apex, mid anterior and anterolateral walls (arrows). Hypokinesis is noted in the corresponding segments in the gated PET images. (E, F) Right (E) and left coronary arteries (F) from the frontal view in selective coronary angiograms. (G, H) Three-dimensional volume rendering of coronary arteries and heart superimposed with color-coded ^{18}FDG images (90–100% of peak uptake coded pink and 0–10% coded black). Green lines indicate intersections with two short-axis planes. The right coronary artery (RCA) and side branches are patent from the right lateral view (G), and septum and inferior wall are viable. In the left lateral view (H), the obtuse marginal artery (OM) is patent, corresponding to normal ^{18}FDG uptake in the supplied lateral wall. In contrast, LAD and the diagonal branch (Diag) are irregularly narrow, corresponding to ^{18}FDG uptake reduction in the anterior and anterolateral walls.

coregistration of PET/CT from a hybrid PET/CT scanner reduces the complexity and allows minimization of the error associated with human intervention. Algorithms combining respiratory and cardiac gated images[19] and CTA acquired during various breathing points could be expected to eliminate manual steps and provide superior accuracy. Here, we reported an interactive interface which allows clear topographical correspondence between the myocardium and coronary arteries. This flexible image display is helpful for clinicians to define the supplying coronary arteries and diseased myocardium. Although the case number was limited, our results have demonstrated the clinical feasibility. In addition, perfusion could provide a closer association to coronary lesions. The 3D fusion technique could additionally provide guidance for an anatomy-based intervention

approach, such as surgical ventricular restoration or molecular intervention.[20] The real value of the combined anatomical and functional approach warrants further investigation.

We present a feasible technique to acquire coronary CTA and PET images and to visualize the fused image data with an interactive interface. This technique is potentially useful in facilitating disease assessment and treatment planning.

Acknowledgments

We are grateful to Mr Chien-Chung Chen for technical assistance in PET/CT acquisition. This study was supported, in part, by a grant (NSC 94-2614-E-002-002) from the National Science Council of Taiwan.

References

1. Huang PJ, Lin LC, Yen RF, et al. Accuracy of biphasic response, sustained improvement and worsening during dobutamine echocardiography in predicting recovery of myocardial dysfunction after revascularization: comparison with simultaneous thallium-201 reinjection SPECT. *Ultrasound Med Biol* 2001;27:925–31.
2. Cerqueria MD, Weissman NJ, Dilsizian V, et al. Standardized myocardial segmentation and nomenclature for tomographic imaging of the heart. *Circulation* 2002;105:539–42.
3. Kalbfleisch H, Hort W. Quantitative study on the size of coronary artery supplying areas postmortem. *Am Heart J* 1977;94:183–8.
4. Hacker M, Jakobs T, Matthiesen F, et al. Comparison of spiral multidetector CT angiography and myocardial perfusion imaging in the noninvasive detection of functionally relevant coronary artery lesions: first clinical experiences. *J Nucl Med* 2005;46:1294–300.
5. Schindler TH, Nitzsche EU, Magosaki N, et al. Myocardial viability in patients with ischemic cardiomyopathy—evaluation by 3D integration of myocardial scintigraphic data and coronary angiographic data. *Mol Imaging Biol* 2004;6:160–71.
6. Mollet NR, Cademartiri F, van Mieghem CAG, et al. High-resolution spiral computed tomography coronary angiography in patients referred for diagnostic conventional coronary angiography. *Circulation* 2005;112:2318–23.
7. Namdar M, Handy, TF, Koepfli P, et al. Integrated PET/CT for the assessment of coronary artery disease: a feasibility study. *J Nucl Med* 2005;46:930–5.
8. Sampson UK, Dorbala S, Limaye A, et al. Diagnostic accuracy of rubidium-82 myocardial perfusion with hybrid positron emission tomography/computed tomography in the detection of coronary artery disease. *J Am Coll Cardiol* 2007;49:1052–8.
9. Nakeura T, Utsunomiya D, Shiraishi S, et al. Three-dimensional cardiac image fusion using new CT angiography and SPECT methods. *AJR Am J Roentgenol* 2005;185:1554–7.
10. Rispler S, Keidar Z, Ghersin E, et al. Integrated single-photon emission computed tomography and computed tomography coronary angiography for the assessment of hemodynamically significant coronary artery lesions. *J Am Coll Cardiol* 2007;49:1059–67.
11. Bax JJ, Beanlands RS, Klocke FJ, et al. Diagnostic and clinical perspectives of fusion imaging in cardiology: is the total greater than the sum of its parts? *Heart* 2007;93:16–22.
12. Slomka PJ. Software approach to merging molecular with anatomic information. *J Nucl Med* 2004;45:36S–45S.
13. Wu YW, Yen RF, Chieng PU, et al. Thallium-201 myocardial perfusion imaging in differentiation of ischemic from nonischemic dilated cardiomyopathy in patients with left ventricular dysfunction. *J Nucl Cardiol* 2003;10:369–74.
14. Wu YW, Huang PJ, Lee CM, et al. Assessment of myocardial viability using F-18 fluorodeoxyglucose/Tc-99m sestamibi dual-isotope simultaneous acquisition SPECT: comparison with Tl-201 stress-reinjection SPECT. *J Nucl Cardiol* 2005;12:451–9.
15. Kuettner A, Kopp AF, Schroeder S, et al. Diagnostic accuracy of multidetector computed tomography coronary angiography in patients with angiographically proven coronary artery disease. *J Am Coll Cardiol* 2004;43:831–9.
16. Lee WJ, Wang YT, Lee HT, et al. The effect of heart rate on the selection of cardiac phases for coronary CT angiography. *Eur Radiol* 2005;15:E34.
17. Austen WG, Edwards JE, Frye RL, et al. A reporting system on patients evaluated for coronary artery disease. Report of the Ad Hoc Committee for Grading of Coronary Artery Disease, Council on Cardiovascular Surgery, American Heart Association. *Circulation* 1975;51:5–40.
18. Di Carli MF, Dorbala S, Hachamovitch R. Integrated cardiac PET-CT for the diagnosis and management of CAD. *J Nucl Cardiol* 2006;13:139–44.
19. Nehmeh SA, Erdi YE, Pan T, et al. Four-dimensional (4D) PET/CT imaging of the thorax. *Med Phys* 2004;31:3179–86.
20. Wagner B, Anton M, Nekolla SG, et al. Noninvasive characterization of myocardial interventions by integrated positron emission tomography and computed tomography. *J Am Coll Cardiol* 2006;48:2107–15.